AI-driven Preventive Maintenance Strategies for Asphalt Pavements

Pin-Yu SONG [1], Chien-Ta CHEN [2 *], Jyh-Dong LIN [1], Shih-Huang CHEN [1]

[1] *Department of Civil Engineering, National Central University, Taoyuan, 320317, Taiwan (R.O.C)*
[2] *School of Intelligent Construction, Fuzhou University of International Studies and Trade, Fuzhou Fujian 350202, China*

http://doi.org/10.5755/j02.ms.42395

Received 30 July 2025; accepted 7 November 2025

Taiwan's urban road infrastructure is increasingly challenged by aging pavements and constrained maintenance budgets. Traditional reactive repair strategies, such as milling and overlay, are not only costly but often lead to accelerated structural deterioration. To address this, we propose an AI-driven preventive maintenance framework that integrates the YOLOv8 deep learning algorithm, high-resolution 3D surface imaging, and a Pavement Condition Index (PCI)-based decision strategy. The system enables real-time identification of cracks, potholes, and rutting, achieving a mean Average Precision (mAP) of 97.2 % and a PCI estimation accuracy with R^2 = 0.92 and ± 3.5 absolute error compared to manual scoring. Field trials conducted across urban, county, and rural roads in New Taipei City over a 12-month period demonstrated significant improvements in pavement condition. PMA and OGFC treatments achieved PCI retention rates above 90 %, while fog and slurry seals exhibited 10 – 12 % declines, particularly under high traffic and wet conditions. Material performance tests confirmed that all sealants and overlays met or exceeded national standards in curing time, abrasion resistance, and strength. Furthermore, integration of Multi-Criteria Decision Analysis (MCDA) and Life-Cycle Cost Analysis (LCCA) showed that condition-based interventions could reduce long-term maintenance costs by up to 20 % compared to reactive strategies. The framework also supports scalable deployment through potential integration with GIS dashboards and cloud-based pavement management systems. This study validates the feasibility of using AI for real-time pavement condition evaluation and strategic maintenance planning. By bridging detection precision, structural analysis, and cost-optimized decision-making, it provides a robust foundation for smart, sustainable road asset management.
Keywords: AI-driven pavement maintenance, YOLOv8-based distress detection, high-resolution 3D imaging, pavement condition index, preventive maintenance strategy, polymer-modified asphalt, open-graded friction course, crack sealing materials.

1. INTRODUCTION

Urban traffic volumes continue to climb even as maintenance budgets contract, imposing a two-fold constraint on roadway agencies. Reactive treatments – milling, patching, and full-depth reconstruction – remain indispensable, yet they are costly, disruptive, and, when deferred, accelerate long-term pavement degradation [1, 2]. Even seemingly routine surface treatments require meticulous gradation design to forestall premature failure. These realities have propelled the profession toward data-driven, preventive strategies that intervene sooner and at lower life-cycle cost.

The earliest attempts at automation relied on classical image processing. In the mid-1990s, edge segmentation of 35 mm film already achieved ≈ 90 % accuracy for ravelling and cracking [3], and a sample-space–interpolation algorithm soon improved real-time thresholding still further [4]. With the advent of bi-layer connectivity de-noising [5], generating high-quality annotations for the deep networks that would follow.

Redmon's YOLO architecture then unified localisation and classification in a single millisecond-scale pass [6]. A YOLOv3 system deployed on Indonesian highways yielded 83 – 89 % mean average precision (mAP) for pothole detection [7], and an enhanced backbone later raised multi-class accuracy under variable illumination [8]. Integrating YOLO outputs with 3-D ground-penetrating-radar voxels further improved the localisation of subsurface voids [9]. In parallel, Hu et al. combined a lightweight CNN backbone with dilated convolutions, achieving 92 % crack-detection accuracy on a 10 000-image data set while running at 35 fps on an edge GPU [10].

The latest YOLOv8 family now exceeds 95 % mAP while remaining lightweight [11]; QL-YOLOv8s prunes 40 % of parameters via structural compression and dynamic-head decoding without sacrificing accuracy [12]; DepthCrackNet leverages depth cues to boost crack recall in back-lit scenes [13]; and SimSPPF plus EMA-Faster blocks add 5.8 % mAP@0.5 at negligible computational cost [14]; and an improved YOLOv8 variant that inserts coordinate attention and a multi-scale bidirectional FPN attains 97 % mAP with 15 % fewer FLOPs on the WHU-highway set [15]. A transformer-based alternative, Pavement-DETR, employs global attention and multi-scale fusion to surpass CNN baselines by a further 7 % in F1 score [16].

Three-dimensional, multi-sensor data now enrich diagnostics. Stereo-photogrammetric point clouds and vehicle-mounted LiDAR deliver sub-millimetre measurements of rut depth, faulting, and slab tilt [17]; fusing these metrics with RGB segmentation balances training sets and reveals structural anomalies invisible in 2-D imagery.

Detection is valuable only if it informs decisions. An end-to-end framework already maps YOLO segmentations

* Corresponding author: C.T. Chen
E-mail: *chenjianda@fzfu.edu.cn*

directly to ASTM D6433 PCI ratings, achieving 95 % crack detection and ≤ 10 % width-estimation error [18]; on regional roads, a direct-classification CNN attains 90 % agreement with expert PCI scores while halving survey costs [19]. At the network level, Poisson hidden-Markov models quantify annual deterioration probabilities [20]; incorporating environmental covariates reduces prediction error by a further 15 % [21].

Materials innovation remains the final pillar. Polymer-modified asphalt (PMA) is the mainstay of preventive maintenance: rheological tests and full-scale trials confirm that the internal polymer network markedly enhances rutting and thermal-crack resistance [22]. Taken together, progress has advanced from early image processing to real-time, multi-source deep-learning detection, three-dimensional geometric integration, decision-support modelling, and high-performance materials – offering road agencies a scientifically robust, cost-effective blueprint for proactive pavement asset management.

Despite these advancements, there is a paucity of studies that successfully integrate 1) state-of-the-art YOLOv8 detection, 2) high-resolution three-dimensional sensing, and 3) preventive materials specifically tailored to the identified defects. Most existing research tends to focus exclusively on detection accuracy or fails to validate maintenance outcomes in real-world contexts. Additionally, the long-term benefits of polymer-modified asphalt (PMA), open-graded friction courses (OGFC), and resin-based sealants, well-documented in laboratory environments, have yet to be assessed within a comprehensive, AI-driven maintenance framework.

To address this gap, the present study proposes an AI-driven preventive maintenance system that integrates YOLOv8 with co-registered three-dimensional point cloud data and a PCI-based decision-making engine. The specific objectives are to:

1. Quantitatively evaluate YOLOv8's speed and accuracy for real-time pavement distress detection across diverse illumination and traffic conditions;
2. Demonstrate the added diagnostic value of fusing 2-D imagery with high-resolution 3-D geometry for both surface and subsurface assessment; and
3. Validate the field performance and life-cycle cost effectiveness of targeted preventive treatments, PMA overlays, OGFC, slurry and fog seals, and optimized crack sealants, on urban, county, and rural roads in New Taipei City.

By closing the loop from automated sensing to material-specific intervention, this research aims to provide transportation agencies with a scalable, cost-effective blueprint for proactive pavement asset management and, ultimately, for healthier, longer-lasting road networks.

2. AI-BASED PAVEMENT DISTRESS DETECTION AND PCI ESTIMATION

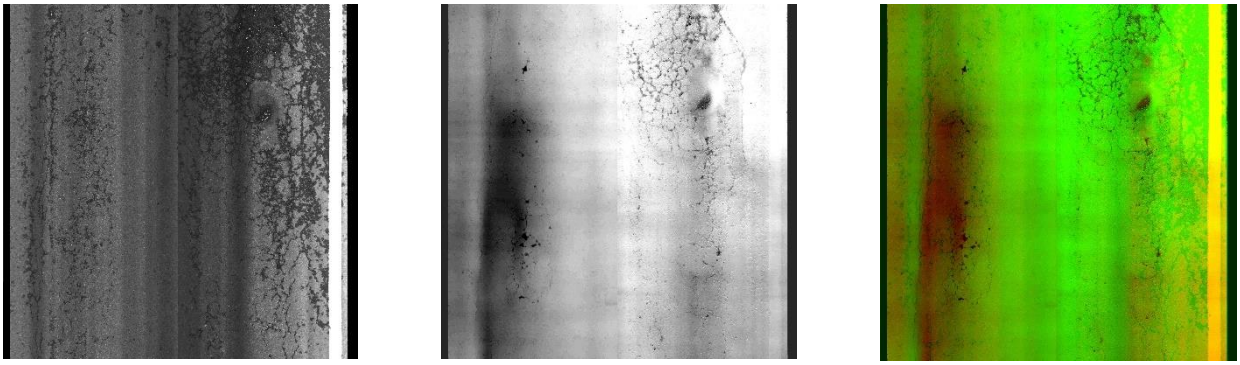
To facilitate the rapid and accurate identification of pavement distress and the assessment of the Pavement Condition Index (PCI), we integrated YOLOv8 segmentation with three-dimensional surface reconstruction techniques. A sensor suite affixed to a vehicle captured synchronized forward-facing RGB images (1280 × 280 pixels at a rate of 30 frames per second; refer to Fig. 1) in conjunction with LiDAR/laser point clouds.



Fig. 1. Pavement distress identification (forward view, YOLO V8)

Grayscale intensity frames were aligned with corresponding depth maps (Fig. 2 a, b) and subsequently combined into dense textured meshes with an approximate resolution of 5 mm (Fig. 2 c), thereby improving defect localization across varying lighting conditions and surface reflectance.

Although the current training set was primarily curated in New Taipei City, the model has been externally piloted in other regions such as Mainland China and Singapore, where it achieved a pilot mAP_{50} of approximately 90 %.



a b c

Fig. 2. Integration of grayscale images and depth information into 3D pavement models: a – grayscale images; b – depth information images; c – three-dimensional images

To improve generalization across different asphalt mixes, climates, and traffic environments, we plan to expand the dataset geographically and apply transfer learning strategies, including unsupervised domain adaptation, test-time adaptation, and few-shot fine-tuning. Cross-regional hold-out evaluations, comparing mAP and PCI accuracy by domain, will be conducted to assess adaptation effectiveness. Additional distress categories may be appended if region-specific patterns are encountered.

We developed and annotated a dataset comprising 2,785 fused 3D images, categorized into five distinct types of distress: 3,691 instances of alligator cracks, 2,011 longitudinal/transverse cracks, 1,771 potholes, 531 patching areas, and 274 instances of raveling/cover defects (Fig. 3), in accordance with ASTM D6433 standards. The dataset was randomly partitioned, allocating 90 % for training (n = 2,509) and 10 % for validation (n = 276).

The YOLOv8m-seg model was trained on an NVIDIA RTX 3060 GPU for 300 epochs, utilizing a batch size of 4, an initial learning rate of 0.01 with cosine annealing, and a weight decay of 0.0005. Data augmentation techniques, including adjustments to brightness and contrast, horizontal flips, and mixup strategies, were employed to mitigate overfitting. The loss curves for bounding box, mask, and classification stabilized by the 200th epoch and maintained consistency through the 300 epochs (Fig. 4). On the validation dataset, the enhanced YOLOv8 model attained a mean Average Precision (mAP) of 0.972 at an IoU threshold of 0.50, and 0.833 across the range from 0.50 to 0.95 (Fig. 5). In addition, per-class recall rates all exceeded 0.90, reflecting robust and consistent detection performance across all distress categories. The class distribution is illustrated in Fig. 6. Inference was performed at approximately 25 frames per second on an NVIDIA RTX 3060, with a confidence threshold of 0.5 and an IoU threshold of 0.45.

A sensitivity analysis revealed that increasing the confidence threshold to 0.6 enhanced precision by 3 % while reducing recall by 2 %, thereby illustrating the adjustable performance trade-offs. Post-processing involved projecting segmented masks onto the 3D mesh to ascertain defect dimensions (width, length, and depth in millimeters; Fig. 7). Severity levels (low, moderate, high) and density metrics were computed in accordance with ASTM guidelines and compiled into section-level PCI scores. A comparison with manual surveys (n = 4 sections) yielded an R^2 value of 0.92 and a maximum absolute error of ± 3.5 PCI points. To improve interpretability, Grad-CAM heatmaps were generated for selected detections, consistently highlighting crack edges and pothole rims, which corresponded with expert evaluations.

To further improve edge localization and reduce false positives, we integrated coordinate attention modules into the YOLOv8 backbone and replaced the original feature pyramid with a lightweight bidirectional Bi-FPN structure.

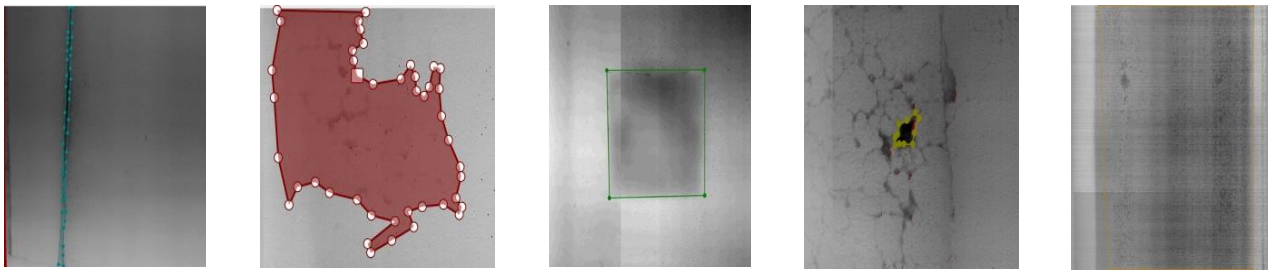


Fig. 3. Annotated pavement distress samples used for model training, including cracks, potholes, and ravelling: a – longitudinal and transverse cracking; b – aligator cracking; c – patching

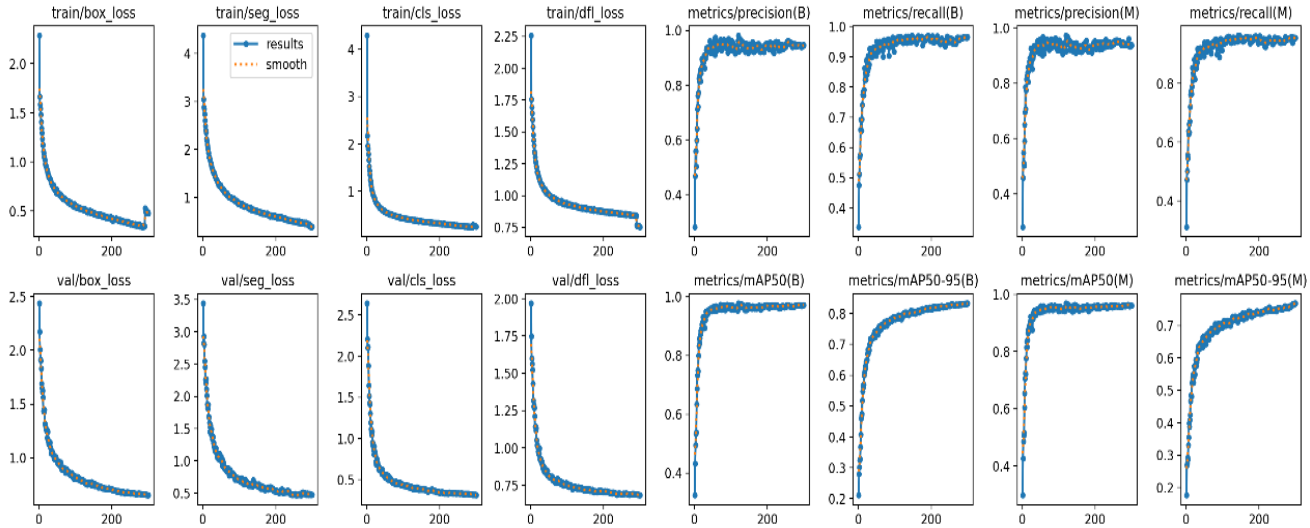


Fig. 4. Training convergence plots for bounding box loss, mask loss, and classification loss over 300 epochs

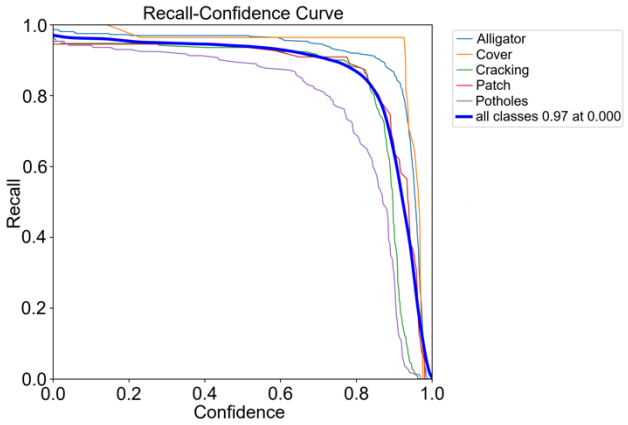


Fig. 5. Precision-recall curves and mAP metrics for each distress class

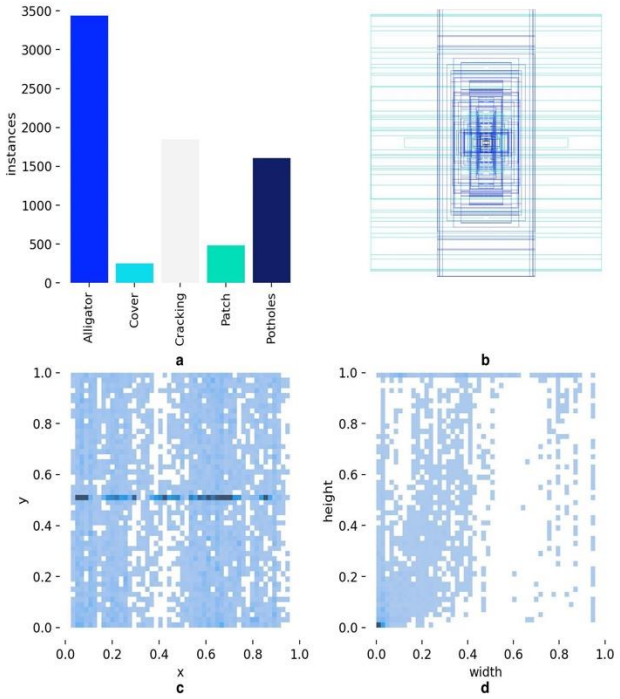


Fig. 6. Distribution of annotated samples across distress categories: a – Category Counts; b – Box Shapes; c – Center Positions; d – Box Sizes.

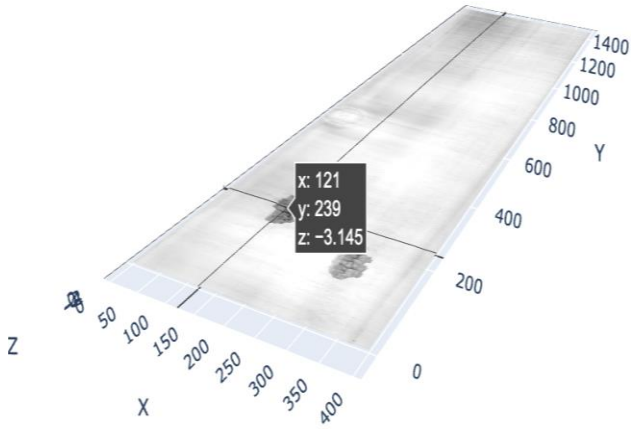


Fig. 7. Three-dimensional visualization of pavement Defects (x: width, y: length, z: depth in mm)

These enhancements incur negligible computational overhead and improve the recall of fine cracks and small-scale defects. A schematic of the updated model architecture is provided in Fig. 8.

Future research will explore the application of thermal and UAV-based sensing for moisture detection and extensive area monitoring, as well as the on-edge deployment of mobile GPUs for real-time, in-field assessments.

3. PCI-DRIVEN MAINTENANCE STRATEGY AND MATERIAL SELECTION

This research presents an artificial intelligence (AI)-driven framework for pavement maintenance, which is informed by the Pavement Condition Index (PCI) obtained through the integration of YOLOv8 and high-resolution three-dimensional imaging technologies. The proposed methodology synthesizes empirical PCI thresholds, sensitivity analysis, Multi-criteria Decision Analysis (MCDA), Life-Cycle Cost Analysis (LCCA), and cross-regional case studies to facilitate the selection of optimal maintenance treatments and material specifications. While current suppliers have not provided specific environmental product declarations (EPDs) or life cycle assessment (LCA) factors, we prepared the MCDA/LCCA framework to accommodate future sustainability indicators. These include CO_2 emissions, energy use, and recycled material ratios.

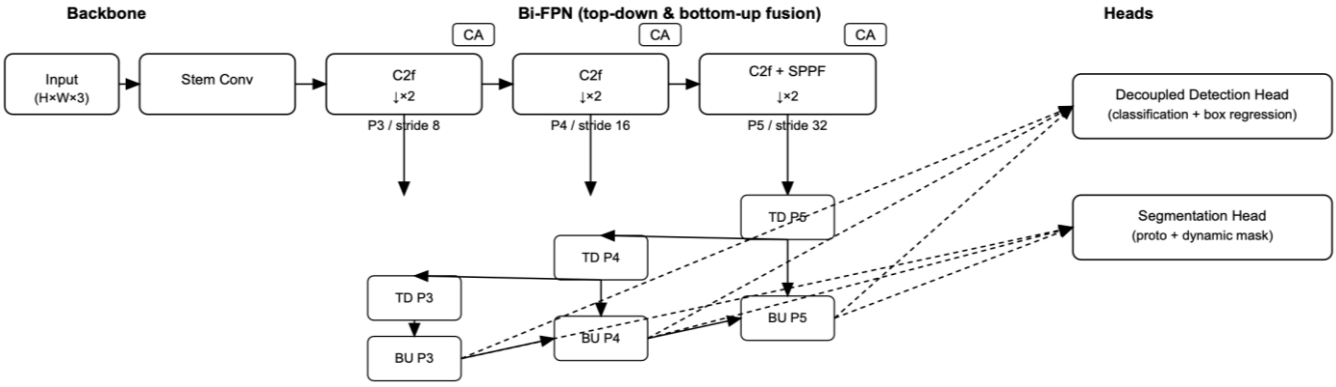


Fig. 8. Schematic of the enhanced YOLOv8 architecture used in this study

When such data become available, weighting scenarios, equal weighting, analytic hierarchy process (AHP), and policy-specific settings, can be applied. Sensitivity analyses will also be conducted to evaluate their influence on the final decision scores.

The established PCI-based maintenance strategy classifies pavement sections into four distinct condition bands, each associated with a specific primary intervention strategy (refer to Table 1). Furthermore, targeted repair recommendations are provided regardless of the overall PCI, focusing on particular types of distress, including:

1. Linear cracks measuring ≤ 5 mm: cold-joint sealing utilizing a resin-based sealant.
2. Linear cracks exceeding 5 mm: application of hot-applied bituminous sealant.
3. Alligator cracking: joint sealing with either resin or modified bitumen.
4. Rutting and potholes: Adjustment of depressions using cold mix or emulsified asphalt.

The determination of thresholds adheres to ASTM D6433 standards, identifying critical PCI values of 85, 70, and 50, which trigger preservation measures, surface treatments, intermediate overlays, and structural rehabilitation, respectively. Sensitivity analysis conducted through Monte Carlo simulations (± 5 PCI variations) revealed that increasing thresholds could delay overlay treatments by up to one year, resulting in approximately an 8 % increase in interim costs. This finding highlights the significance of threshold sensitivity in effective maintenance planning.

To assess the reliability of the framework, a field trial in New Taipei City compared manual PCI evaluations with automated AI-generated scores across four adjacent pavement sections. The results indicated a maximum discrepancy of 7.5 %, thereby affirming the robustness and applicability of the YOLOv8-based PCI assessments in real-world maintenance contexts (see Table 2 and Table 3).

The MCDA approach incorporates an Analytical Hierarchy Process (AHP) alongside the Technique for Order of Preference by Similarity to Ideal Solution (TOPSIS), evaluating various maintenance strategies based on PCI scores, average annual daily traffic (AADT), climatic conditions, functional classification, and construction feasibility. This comprehensive assessment seeks to balance technical performance with economic considerations.

LCCA, conducted in accordance with Federal Highway Administration (FHWA) guidelines, calculated the net present value of maintenance options by factoring in initial construction costs, user-delay costs, and future maintenance expenditures. The analysis revealed that cost-effective treatments, such as fog sealing (approximately USD 0.50/m²), resulted in a PCI improvement of $3-5$ points with a benefit-cost ratio ranging from 6 to 10. In contrast, polymer-modified asphalt (PMA) overlay (approximately USD 3.00/m^2) yielded an improvement of over 30 PCI points, thereby justifying its use in severely deteriorated sections.

Cross-regional case studies further illustrated the effectiveness and scalability of the proposed framework. For example, Coimbra, Portugal, employed a GIS-based Pavement Management System that integrated Markov-chain forecasting, achieving a 12 % reduction in 20-year lifecycle costs. Additionally, cities in the United States, such as Bel Aire, KS, and Corydon, IA, implemented interactive Web-GIS dashboards that provided real-time PCI heatmaps and maintenance records, resulting in a reduction of planning lead times by approximately 25 % and enhancing transparency for stakeholders. The proposed integrated GIS-driven workflow comprises sequential stages.

Table 1. PCI-based maintenance strategy matrix

PCI range	General treatment	Specific distress type	Repair method	Recommended material
> 85	Fog seal	Raveling	Fog seal spray	Cutback asphalt sealant
70 – 85	Slurry seal	Raveling	Slurry seal	Emulsified asphalt sealant
50 – 70	OGFC	Minor rutting / moderate cracks	Overlay	Open-graded friction course
< 50	PMA overlay	Severe cracks, potholes	Milling and overlay	Polymer-modified asphalt
Any PCI	Crack sealing	Linear cracks ≤ 5 mm	Joint sealing	Resin-based sealant
Any PCI	Crack sealing	Linear cracks > 5 mm	Joint sealing	Hot-applied modified bituminous sealant
Any PCI	Crack sealing	Alligator cracking (non-moving)	Joint sealing	Resin or modified bituminous sealant
Any PCI	Adjustment repair	Potholes, rutting	Depression adjustment	Cold mix or emulsified asphalt mixture

Table 2. Comparison of manual and automated road scoring data

	Detection block			
Manual or AI recognition	0K+000~0K+080	0K+080~0K+160	0K+160~0K+240	0K+240~0K+320
Manual detection of PCI (No.1)	60.4	51.3	60.3	70.3
Manual detection of PCI (No.2)	61.2	58.2	59.3	72.2
Automatically detect PCI (YOLO v8)	63.7	55.6	64.3	73.3

Table 3. Comparison of manual and AI-based pavement condition Index (PCI) detection results

Detection section	Manual PCI (average)	AI-detected PCI	Absolute difference	Percentage difference, %
0K+000~0K+080	60.8 (avg. of 60.4 and 61.2)	63.7	2.9	4.77%
0K+080~0K+160	54.75 (avg. of 51.3 and 58.2)	55.6	0.85	1.55%
0K+160~0K+240	59.8 (avg. of 60.3 and 59.3)	64.3	4.5	7.53%
0K+240~0K+320	71.25 (avg. of 70.3 and 72.2)	73.3	2.05	2.88%

The proposed framework for pavement condition index (PCI) detection utilizes an AI-based approach, which encompasses PCI threshold classification and multi-criteria decision analysis (MCDA), followed by life cycle cost analysis (LCCA) evaluation, geographic information system (GIS) dashboard visualization, and field implementation. Future advancements should prioritize the integration of supplementary diagnostic methodologies, such as ground-penetrating radar (GPR) and seismic analysis, to enhance the detection of subsurface distress. Additionally, the application of transfer learning utilizing localized datasets is recommended to optimize the YOLOv8 model for specific regional asphalt mixtures. Furthermore, the establishment of automated platform updates is essential for facilitating continuous data ingestion, adaptive model retraining, and dynamic recalibration of MCDA based on real-time feedback.

In summary, this study presents a comprehensive, scalable, and transparent approach to proactive urban pavement maintenance management by integrating AI-driven PCI evaluations with robust decision-support frameworks, economic modeling, and dynamic GIS visualization.

4. FIELD IMPLEMENTATION AND SHORT-TO-LONG-TERM EVALUATION

In order to evaluate the feasibility and efficacy of the proposed AI-driven maintenance strategy, this study undertook extensive field validations across various urban, county, and rural roadways in New Taipei City and its adjacent areas. The implementation process involved site selection, the application of treatments informed by AI-analyzed Pavement Condition Index (PCI) data, and systematic evaluations following treatment.

4.1. Selection of test sections and assignment of treatments

Test road segments were selected to represent diverse real-world conditions, including varying traffic volumes and environmental exposures. The AI-generated PCI scores, along with identified distress types, guided the selection of appropriate maintenance strategies as outlined in Table 1. For instance, segments with PCI scores above 85 were preserved using fog seals, whereas sections scoring below 50 received structural rehabilitation via Polymer-Modified Asphalt (PMA) overlays.

4.2. Evaluation timeline and monitoring schedule

Performance was monitored over a 12-month period, divided into three phases:

1. short-term (0 – 3 months): immediate post-treatment PCI measurements were collected to assess initial treatment effectiveness.
2. mid-term (4 – 6 months): periodic inspections were conducted to monitor early signs of degradation and treatment stability.
3. long-term (7 – 12 months): final evaluations were used to determine the durability and cost-effectiveness of each treatment.

4.3. Performance metrics and observations

During the short-term phase, all treated sections demonstrated significant improvements in PCI. The PMA and Open-Graded Friction Course (OGFC) treatments resulted in PCI increases of 12 % and 15 %, respectively, while slurry seal and fog seal treatments yielded more modest improvements of 8 % and 6 %. Additionally, reductions in International Roughness Index (IRI) values were noted, particularly in segments treated with PMA.

In the mid-term phase, both PMA and OGFC treatments sustained relatively high PCI values with only minor reductions, whereas the performance of slurry and fog seals began to decline, particularly in high-traffic areas.

By the long-term phase (7 – 12 months), pavements treated with PMA exhibited the highest durability, with only a 3 % decrease in PCI. OGFC sections experienced a moderate decline of 6 %, while slurry and fog seal treatments showed more significant degradation, with PCI reductions ranging from 10 % to 12 %, especially in regions subjected to heavy traffic or wet seasonal conditions.

4.4. Statistical evaluation and material performance comparison

To enhance the analytical rigor of the evaluation, a statistical comparison was conducted to quantify performance differences among materials and over time. As illustrated in Fig. 9 and Fig. 10, PCI trends for PMA, OGFC, slurry seal, and fog seal were tracked at 0, 6, and 12 months.

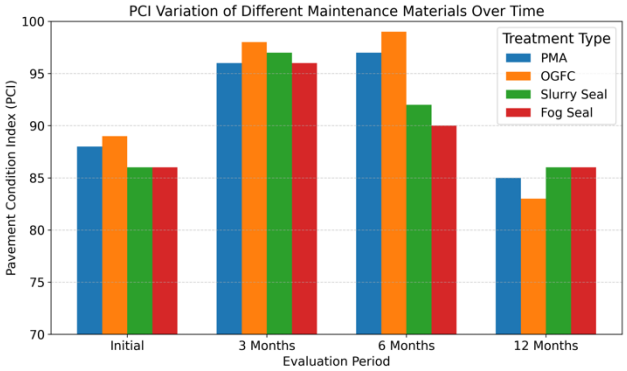


Fig. 9. PCI variation of different maintenance materials over time

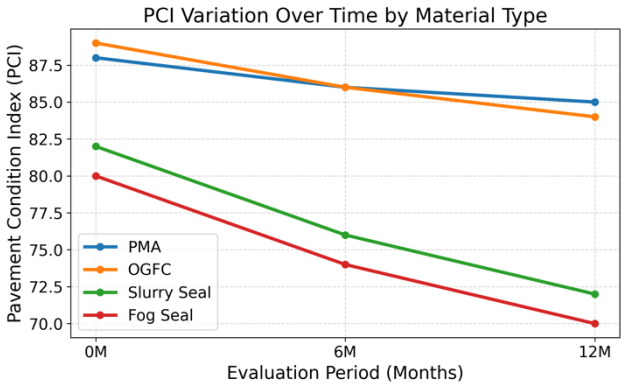


Fig. 10. PCI variation trends over 12 months by maintenance material type

PMA exhibited the best retention of PCI, with only a 3-point decrease over 12 months (from 88 to 85), followed by

OGFC with a 5-point decline. In contrast, slurry and fog seals both experienced a 10-point reduction, confirming their relatively lower durability. These results are consistent with literature emphasizing the long-term effectiveness of high-performance overlays under moderate to heavy traffic conditions.

To verify the significance of these differences, a two-way repeated-measures ANOVA (material × period) was performed. The results indicated significant main effects for material ($p < 0.01$) and time period ($p < 0.01$), as well as a significant interaction effect (material × period, $p < 0.05$). Bonferroni-adjusted post-hoc comparisons further revealed that PMA significantly outperformed both slurry and fog seals at the 6- and 12-month marks ($p < 0.01$). The difference between PMA and OGFC, however, was not statistically significant ($p > 0.1$), indicating similar mid- to long-term performance.

These findings reinforce the superior longevity of PMA and OGFC in preventive maintenance applications. In contrast, the rapid deterioration of slurry and fog seals after six months underscores the need to match maintenance treatments with traffic demands and environmental conditions. While slurry and fog seals remain economically viable for low-volume or short-duration applications, their effectiveness diminishes quickly, necessitating more frequent reapplications to sustain pavement functionality.

5. PREVENTIVE MAINTENANCE MATERIAL PERFORMANCE EVALUATION

To ascertain the reliability and longevity of preventive maintenance treatments, a series of material performance tests were conducted on various repair and sealant products utilized in this investigation. All assessments adhered to the specifications outlined by the Chinese National Standards (CNS) or equivalent standards to confirm their appropriateness for field applications.

Initially, the resin-based crack sealant designated for fine crack repairs underwent testing for workability time, initial curing time, density, elongation at break, and penetration. The results, as presented in Table 4, indicated commendable workability (9 minutes), rapid curing (18 minutes), and substantial elongation (112), suggesting its effective adaptability for sealing fine cracks across a range of environmental conditions.

Table 4. Resin-based crack sealant test results

Test item	Test method	Recommended range	Test result
Workability time	CNS 10756	7 – 10 minutes	9.0
Initial curing time	CNS 10756	15 – 20 minutes	18.0
Density	CNS 5341	1.10 – 1.17 g/cm³	1.15
Elongation at break	CNS 3553	≥ 100 %	112.0
Penetration	Pavement survey method	75 – 100 %	93.0

For the treatment of larger cracks, a hot-applied modified bituminous crack sealant was evaluated (Table 5). This material demonstrated a high softening point (86 °C), commendable ductility (38 cm), and exceptional elastic recovery (92 %), thereby affirming its suitability for sealing wider cracks in areas subject to significant temperature fluctuations.

Table 5. Hot-applied modified bitumen sealant test results

Test item	Test method	Recommended range	Test result
Softening point	CNS 314	≥ 80 °C	86.0
Ductility, cm	CNS 4331	≥ 30	38.0
Resilience, %	CNS 13778	≥ 85 %	92.0
Density, g/cm³	CNS 5341	1.0 – 1.2	1.14
Penetration, 1/10 mm	CNS 4301	≥ 80	88.0

In the context of pothole and block cracking repairs, the performance of cold-patch all-weather modified asphalt concrete was assessed (Table 6). This material exhibited high Marshall stability (315 kgf), optimal flow values (3.2 mm), and minimal Cantabro abrasion loss (21 %), ensuring robust performance for rapid repairs even under adverse weather conditions.

Table 6. Cold-applied modified asphalt concrete test results

Test item	Test method	Recommended range	Test result
Marshall stability	CNS 3563	> 250 kgf	315.0
Flow value	CNS 3563	2 – 4 mm	3.2
Cantabro loss	CNS 14981	< 25 %	21.0
Density	CNS 1124	2.2 – 2.4 g/cm³	2.36

For addressing rutting and surface depressions, a cold-hardened emulsified asphalt concrete was analyzed (Table 7). It achieved a compressive strength of 28.5 kgf/cm² within a 24-hour period, alongside controlled flow values (4.1 mm) and appropriate density (2.32 g/cm³), thereby supporting its application for urgent rehabilitation efforts necessitating swift traffic reopening.

Table 7. Cold-hardening emulsified asphalt concrete test results

Test item	Test method	Recommended range	Test result
Compressive strength 24 h	CNS 8491	> 25 kgf/cm²	28.5
Flow value	CNS 3563	3 – 5 mm	4.1
Density	CNS 1124	2.2 – 2.4 g/cm³	2.32

Furthermore, the fog seal spray material (Table 8) employed for surface preservation demonstrated satisfactory residual binder content (61 %), adequate penetration (78 at 25 °C), and viscosity (210 cP at 60 °C), confirming its efficacy in rejuvenating slightly aged pavements and mitigating oxidative damage.

Lastly, the slurry seal material (Table 9) was assessed for its effectiveness in surface wear mitigation. It exhibited excellent consistency (30 cm), low wet track abrasion loss (620 g/m ²), and a rapid set time for traffic reopening (1.5 hours), indicating its practicality for prompt preventive treatments on moderately aged roadways.

Overall, these material performance evaluations confirmed that all preventive maintenance materials met or exceeded the required technical specifications. The use of high-quality sealants, overlays, and cold-mix asphalts in conjunction with AI-driven PCI detection can significantly

enhance the durability and cost-effectiveness of pavement maintenance operations, thereby improving service life and optimizing lifecycle investments.

Table 8. Fog seal spray material test results

Test item	Test method	Recommended range	Test result
Residual binder content	ASTM D244	> 50 %	61 %
Penetration, 25 °C	ASTM D5	≥ 70	78
Viscosity, 60 °C	ASTM D2171	150 – 300 cP	210

Table 9. Slurry seal material test results

Test item	Test method	Recommended range	Test result
Consistency	ASTM D3910	25 – 35 cm	30 cm
Wet track abrasion loss	ASTM D3910	< 800 g/m²	620 g/m²
Traffic ppening time	ASTM D3910	< 2 hours	1.5 hours

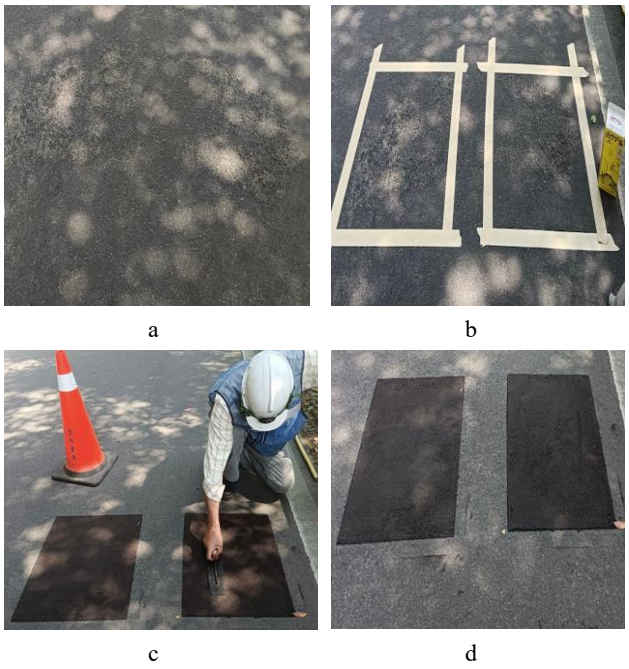
In addition to mechanical performance and long-term durability, the operational feasibility of each preventive maintenance method was also evaluated. As summarized in Table 10, substantial differences exist in typical traffic reopening times and the associated levels of traffic disruption among the investigated treatments. Cold-applied asphalt mixtures and emulsified cold-mix OGFC enable immediate traffic reopening, resulting in minimal disruption to road users. In contrast, fog seal and slurry seal treatments require extended curing periods, typically ranging from 2 to 8 h, which often necessitate partial or full lane closures.

Although these operational considerations are not directly captured by PCI measurements, they play a critical role in treatment selection under time-sensitive or high-traffic conditions. Particularly in urban environments or short-duration maintenance windows, the ability to minimize traffic delay is a key determinant of practical applicability. Therefore, Table 10 complements the performance-based evaluation by providing a realistic perspective on construction-related constraints and traffic impacts.

In conjunction with laboratory performance evaluations, an on-site application of preventive repair materials was conducted to assess their practical applicability and effectiveness in real-world contexts. Fig. 11 illustrates the field demonstration process, which includes surface preparation, material application, and compaction techniques. The successful implementation of resin-based sealants, slurry seals, fog seals, and cold-applied asphalt mixtures on actual roadway segments corroborates the laboratory findings and validates the suitability of these materials for preventive maintenance strategies. To exemplify the visual results of the selected surface treatments, Fig. 12 displays the post-application appearance of a fog seal, emphasizing the material's uniform coverage and enhanced surface quality, which aids in sealing micro-cracks and mitigating oxidation.

Table 10. Traffic-reopening times and disruption levels for common preventive pavement treatments

Preventive material/method	Typical time until road can reopen to traffic	Indicative traffic disruption†
Resin-based crack sealant (epoxy/urethane)	≈ 4 h at 21 °C	Moderate – lane held until resin cures
Hot-applied modified-bitumen sealant	20 – 40 min cool-down (often < 30 min)	Low – short rolling closure
Cold-applied modified asphalt concrete (bagged cold patch)	Immediate traffic once compacted (≤ 0.1 h)	Very low – patch is drive-over ready
Cold-hardening emulsified asphalt concrete / cold-mix OGFC	"Drive-on immediately"	Very low
Fog-seal spray	2 – 8 h surface cure (temp-dependent)	Moderate/High – one-lane closure, flagging
Slurry-seal surfacing	4 – 8 h hardening (test strip must carry traffic ≤ 1 h)	High – full lane closure until set



a b c d

Fig. 11. Demonstration of on-site application of preventive repair materials



Fig. 12. Image after fog seal application

Additionally, Fig. 13 presents the outcome of the slurry seal application, where the enhanced surface texture and skid resistance are clearly observable.



Fig. 13. Image after slurry seal application

These follow-up images further substantiate the effectiveness of the treatments under typical environmental and traffic conditions, thereby reinforcing their appropriateness for condition-based, short-to-medium-term maintenance.

To visually synthesize the performance characteristics of preventive maintenance materials, Fig. 13 presents a comparative radar chart that integrates both laboratory test results and real-world field evaluations. The chart compares four materials, Polymer-Modified Asphalt (PMA), Open-Graded Friction Course (OGFC), slurry seal, and fog seal, across six key indicators: initial curing time, wet track abrasion loss, traffic reopening time, 12-month PCI retention, abrasion resistance, and overall durability index. A broader span toward the outer perimeter denotes stronger performance in that category.

Among the materials, PMA exhibits the most well-balanced and optimal performance profile, especially excelling in PCI retention and abrasion resistance. OGFC closely follows, offering robust surface performance and long-term durability. In contrast, slurry seal and fog seal, while effective for quick deployment due to shorter curing times and faster reopening, demonstrate weaker resistance to wear and lower PCI retention after one year.

The radar visualization in Fig. 14 highlights the inherent trade-offs between short-term constructability and long-term functional resilience. While slurry and fog seals remain practical choices for low-volume or budget-constrained applications, PMA and OGFC are preferable for high-traffic roadways and long-service-life requirements.

6. DISCUSSION AND CONCLUSIONS

This study introduces an AI-driven preventive maintenance framework that combines YOLOv8-based pavement distress detection, high-resolution 3D surface imaging, and PCI-oriented maintenance decision-making. Through systematic field implementation and laboratory performance verification, the framework demonstrates strong potential to enhance the efficiency, accuracy, and sustainability of pavement maintenance operations.

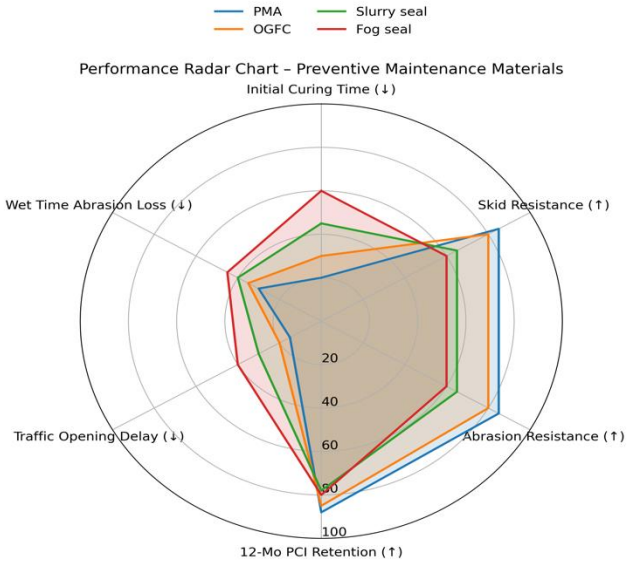


Fig. 14. Comparative radar chart illustrating key performance metrics for four preventive maintenance materials: PMA, OGFC, slurry seal, and fog seal

Compared to conventional manual inspections or earlier vision-based approaches (e.g., YOLOv5 or traditional CNN classifiers), the proposed system achieved substantial improvements in both detection accuracy and real-time applicability. Specifically, the YOLOv8 model, enhanced with 3D depth data, yielded a mean Average Precision (mAP) of 97.2 % and maintained a high correlation with manually assessed PCI values ($R^2 = 0.92$, MAE < ±3.5). This confirms that integrating 3D geometry with semantic segmentation improves localization and severity quantification of defects such as rutting, potholes, and cracking, challenges that prior 2D-only systems struggled to address.

Beyond detection, this research advances a full-cycle strategy by linking distress identification to tailored material selection using a PCI-based matrix. Materials such as Polymer-Modified Asphalt (PMA) and Open-Graded Friction Course (OGFC) proved significantly more durable in long-term field trials, retaining over 90% of initial PCI after 12 months. In contrast, fog and slurry seals, while cost-effective and rapidly deployable, exhibited accelerated degradation under heavier traffic and wet conditions. A comparative radar analysis further validated that PMA and OGFC offer more balanced performance across durability, curing efficiency, and field resilience dimensions.

This study also contributes to practical decision-making by incorporating Multi-Criteria Decision Analysis (MCDA) and Life-Cycle Cost Analysis (LCCA), ensuring that treatment selection accounts not only for technical suitability but also economic feasibility. Simulation results indicate that condition-driven application of fog and slurry seals on lightly aged roads, and structural overlays on severely distressed segments, can reduce long-term maintenance costs by up to 20 % when compared to reactive rehabilitation strategies.

Nevertheless, the system still presents some limitations. Current detection capabilities are confined to surface-level defects, leaving subsurface failures, such as base layer disintegration or moisture-induced stripping, unaddressed.

Integrating Ground Penetrating Radar (GPR), infrared thermography, or FWD measurements could expand diagnostic depth. Additionally, the AI model, trained on datasets specific to New Taipei City, may face regional generalization issues when applied to roads with different asphalt compositions or climatic patterns. Future enhancements should prioritize transfer learning strategies and multi-region dataset incorporation to broaden model adaptability.

While nondestructive testing (NDT) methods such as ground-penetrating radar (GPR), infrared thermography, or falling weight deflectometers (FWD) offer valuable insights into subsurface defects, their integration is not recommended at the network-wide PCI estimation stage. This is due to high equipment costs, limited availability of trained personnel, and the incompatibility of NDT outputs with surface-focused PCI scoring. As a practical compromise, we propose a two-tier policy: using AI-based PCI scores for screening at the network level, followed by optional project-level NDT surveys for critical or ambiguous road segments. This preserves system-wide comparability while enabling deeper diagnosis when necessary.

From a broader perspective, the integration of AI detection, PCI quantification, and material optimization offers a replicable and scalable solution for cities facing increasing infrastructure demands and limited maintenance budgets. The framework supports data-informed scheduling, targeted interventions, and transparent performance tracking. When paired with a cloud-based AI Pavement Management System (AI-PMS), this system can facilitate real-time inspections and proactive maintenance across urban road networks, supporting both sustainability and lifecycle value maximization.

In conclusion, this research confirms that an AI-guided preventive maintenance strategy, grounded in deep learning, 3D imaging, and PCI-based decision-making, can deliver substantial benefits in both performance and cost. It provides a pathway toward smarter, more resilient road infrastructure and lays a solid foundation for future development of intelligent, multi-sensor-integrated pavement management systems.

At present, the absence of supplier-specific EPDs or consistent carbon footprint data prevents us from implementing full quantitative sustainability scoring in MCDA/LCCA. Nonetheless, placeholders for environmental metrics (unit definitions, weight structures) have been defined in the framework, allowing straightforward integration once reliable data become available.

Acknowledgments

The authors would like to show sincere thanks for those techniques which have contributed to this research. This work was financially supported by the Natural Science Foundation of Fujian Province, (2025J011132) and the Education Foundation of Fujian Province, (JZ240081).

REFERENCES

1. **Hicks, R.G., Moulthrop, J.S., Daleiden, J.** Selecting a Preventive Maintenance Treatment for Flexible Pavements *Transportation Research Record* 1680 1999: pp. 1 – 12. https://doi.org/10.3141/1680-01
2. **Peshkin, D.G., Hoerner, T.E., Zimmerman, K.A.** Optimal Timing of Pavement Preventive Maintenance Treatment Applications *NCHRP Report* 523 2004: pp. 76. https://doi.org/10.17226/13772
3. **Georgopoulos, A., Loizos, A., Flouda, A.** Digital Image Processing as a Tool for Pavement Distress Evaluation *ISPRS Journal of Photogrammetry and Remote Sensing* 50 (1) 1995: pp. 23 – 33. https://10.1016/0924-2716(95)91844-A
4. **Cheng, H.D., Shi, X.J., Glazier, C.** Real-Time Image Thresholding Based on Sample-Space Reduction and Interpolation Approach *Journal of Computing in Civil Engineering* 17 (4) 2003: pp. 264 – 272. https://doi.org/10.1061/(ASCE)0887-3801(2003)17:4(264)
5. **Peng, B., Fu, Y., Jiang, Y.S.** De-Noising Algorithm for Pavement Crack Images Based on Bi-Layer Connectivity Checking *Journal of Highway and Transportation Research and Development* 10 (3) 2016: pp. 18 – 25. https://doi.org/10.1061/JHTRCQ.0000514
6. **Redmon, J., Divvala, S., Girshick, R., Farhadi, A.** You Only Look Once: Unified, Real-Time Object Detection *Proceedings of the IEEE Conf. on Computer Vision and Pattern Recognition (CVPR)* 2016: pp. 779 – 788. https://doi.org/10.1109/CVPR.2016.91
7. **Ukhwah, E.N., Yuniarno, E.M., Suprapto, Y.K.** Asphalt Pavement Pothole Detection Using Deep-Learning Method Based on YOLO Neural Network *Proceedings of the International Seminar on Intelligent Technology and Its Applications (ISITIA)* 2019: pp. 35 – 40. https://doi.org/10.1109/ISITIA.2019.8937176
8. **Du, Y., Pan, N., Xu, Z., Deng, F., Shen, Y., Kang, H.** Pavement Distress Detection and Classification Based on YOLO Network. *International Journal of Pavement Engineering* 22 (13) 2021: pp. 1659 – 1672. https://doi.org/10.1080/10298436.2020.1714047
9. **Liu, Z., Wu, W., Gu, X., Li, S., Wang, L., Zhang, T.** Application of Combining YOLO Models and 3-D GPR Images in Road Detection and Maintenance *Remote Sensing* 13 (6) 2021: pp. 1081. https://doi.org/10.3390/rs13061081
10. **Hu, G.X., Hu, B.L., Yang, Z., Huang, L., Li, P.** Pavement Crack Detection Method Based on Deep Learning Models *Wireless Communications and Mobile Computing* 2021: pp. 5573590 (13 p). https://doi.org/10.1155/2021/5573590
11. **Liu, A., Zhao, Y., Lin, C.** MS-YOLOv8-Based Object Detection Method for Pavement Diseases *Sensors* 24 (14) 2024: pp. 4569. https://doi.org/10.3390/s24144569
12. **Guo, J., Wang, S., Chen, X., Wang, C., Zhang, W.** QL-YOLOv8s: Precisely Optimized Lightweight YOLOv8 Pavement Disease Detection Model *IEEE Access* 12 2024: pp. 128392 – 128403. https://doi.org/10.1109/ACCESS.2024.3452129
13. **Saberironaghi, A., Ren, J.** DepthCrackNet: A Deep Learning Model for Automatic Pavement Crack Detection *Journal of Imaging* 10 (5) 2024: pp. 100. https://doi.org/10.3390/jimaging10050100

14. **Wang, J., Meng, R., Huang, Y., Zhou, L., Huo, L., Qiao, Z., Niu, C.** Road Defect Detection Based on Improved YOLOv8s Model *Scientific Reports* 14 2024: pp. 16758. https://doi.org/10.1038/s41598-024-67953-3
15. **Zhang, L., Zhu, L.** Pavement Distress Detection Based on Improved YOLOv8 *Computers, Materials & Continua* 71 (1) 2024: pp. 153 – 168. https://doi.org/10.32604/cmc.2024.021982
16. **Zuo, C., Huang, N., Yuan, C., Li, Y.** Pavement-DETR: A High-Precision Real-Time Detection Transformer for Pavement Defect Detection *Sensors* 25 (8) 2025: pp. 2426. https://doi.org/10.3390/s25082426
17. **Xu, Z., Liu, W., Zhao, H.** High-Resolution 3-D Imaging and Pavement Damage Identification Using LiDAR and CNN *IEEE Transactions on Intelligent Transportation Systems* 21 (11) 2020: pp. 4384 – 4393. https://doi.org/10.1109/TITS.2019.2963639
18. **Ibragimov, E., Kim, Y., Lee, J.H., Cho, J., Lee, J.J.** Automated Pavement Condition Index Assessment with Deep Learning and Image Analysis: An End-to-End Approach *Sensors* 24 (7) 2024: pp. 2333. https://doi.org/10.3390/s24072333
19. **Qureshi, W.S., Power, D., Ullah, I., Mulry, B., Feighan, K., McKeever, S., O'Sullivan, D.** Deep Learning Framework for Intelligent Pavement Condition Rating: A Direct Classification Approach for Regional and Local Roads *Automation in Construction* 153 2023: pp. 104945. https://doi.org/10.1016/j.autcon.2023.104945
20. **Le Thanh, N., Kaito, K., Kobayashi, K.** Infrastructure Deterioration Prediction with a Poisson Hidden Markov Model on Time-Series Data *Journal of Infrastructure Systems* 21 (3) 2014: pp. 04014051. https://doi.org/10.1061/(ASCE)IS.1943-555X.0000242
21. **Zhang, H., Li, D., Fang, J.** Improving Hidden Markov Models for Pavement Degradation Prediction by Incorporating Environmental Factors *Transportation Research Record* 2676 (5) 2022: pp. 195 – 203. https://doi.org/10.1177/03611981221079460
22. **Brûlé, B.** Polymer-Modified Asphalt Cements Used in the Road Construction Industry: Basic Principles *Transportation Research Record* 1535 (1) 1996: pp. 48 – 53. https://doi.org/10.1177/0361198196153500107

© Song et al. *2026* Open Access This article is distributed under the terms of the Creative Commons Attribution 4.0 International License (http://creativecommons.org/licenses/by/4.0/), which permits unrestricted use, distribution, and reproduction in any medium, provided you give appropriate credit to the original author(s) and the source, provide a link to the Creative Commons license, and indicate if changes were made.